Journal of Materials Research and Technology 33 (2024) 6251–6262

Contents lists available at ScienceDirect

Journal of Materials Research and Technology

journal homepage: www.elsevier.com/locate/jmrt

Rheology study of the starch gelatinization to understand the hematite depression process

Elaine Cristina Andrade [a], Jean Carlo Grijó Louzada [b], Saeed Chehreh Chelgani [c,d,*], Laurindo de Salles Leal Filho [a]

[a] Department of Mining and Petroleum Engineering, Polytechnic School, University of São Paulo, Brazil
[b] Geosciences and Engineering Institute, Federal University of Southern and Southeastern Pará, Brazil
[c] Minerals and Metallurgical Engineering, Swedish School of Mines, Department of Civil, Environmental and Natural Resources Engineering, Luleå University of Technology, Luleå, Sweden
[d] Wallenberg Initiative Materials Science for Sustainability, Department of Civil, Environmental and Natural Resources Engineering, Swedish School of Mines, Luleå University of Technology, Luleå, Sweden

ARTICLE INFO

Handling editor: M Meyers

Keywords:
Starch gel
Hematite depression
Rheology
Fluid-like behavior
Solid-like behavior

ABSTRACT

Gelatinization of starch by NaOH is an essential stage for this depressant preparation to enhance its water solubility through the reverse cationic flotation. No investigation has explored the rheology of the starch gelatinization to demonstrate the hematite depression completeness. To fill the gap, this study examined the influence of a wide range of SNMRs (3:1, 5:1, 7:1, 9:1) to explore the efficiency of the gelatinization process. The main aim was to highlight how starch gel preparation can influence hematite depression in cationic reverse flotation. The steady and dynamic shear rheological measurements plus optical micrographs were assessed for the starch gel gelatinization process for different SNMR conditions. Various experiment outcomes indicated that through the starch gelatinization by SNMR>6:1, the solubilization did not occur completely (due to the presence of some pristine granules) and the gels exhibited solid-like behavior, as evidenced by $K' > K''$, $\tan\delta < 1$, $\lambda \geq 94.3$s, and $\eta_0 \geq 32.0$ Pa s. The incomplete release of AP macromolecules into the solution was the cause of the poor hematite depression efficiency. Pretreating starch by SNMR ≤5:1 indicated a full release of both AM and AP species to the solution since the gels showed fluid-like behavior with $K' < K''$, $\tan\delta > 1$, $\lambda \leq 0.7$s, and $\eta_0 \leq 2.4$ Pa s. However, the excessive alkalinity promoted a reduction in the hydrodynamic size of macromolecules. These findings explain the better efficiency of SNMR = 5:1 to depress hematite compared to SNMR = 3:1. In general, starch preparation with SNMR = 6:1 marked the onset of the sol-gel transition, and the gels exhibited a balance between fluid-like behavior and solid-like behavior.

1. Introduction

Starch is an important flotation depressant that has been used in the concentration of iron ores through the reverse cationic flotation separation of quartz at pH > 9.5 [1–7]. Starch is a natural biopolymer (polysaccharide) composed predominantly of amylose (AM) and amylopectin (AP) in contents that largely depend on its botanic source, such as corn (75% AP + 25% AM), cassava (76% AP + 24% AM), potato (70% AP + 30% AM) [8–12]. AM is a coiled linear structure with α-(1 → 4) glucoside bonds and a molecular weight of 10^5–10^6 g/mol. In addition, AP is formed by α-*D* glucose units joined together with α-(1 → 4) and α-(1 → 6) bonds in a highly branched structure exhibiting a molecular weight of 10^7–10^9 g/mol [1,12–17].

Since starch granules are naturally insoluble in cold water, the ore dressing plants usually accomplish their gelatinization with sodium hydroxide (NaOH) before flotation by using values of Starch:NaOH Mass Ratio (SNMR) varying in the range 3:1 ≤ SNMR ≤ 6:1. However, a recent publication indicated a higher effective hematite depression by corn starch prepared at SNMR = 5:1 compared to other values (3:1, 7:1, and 9:1) [18]. This process occurred potentially due to a complete release of

* Corresponding author. Minerals and Metallurgical Engineering, Swedish School of Mines, Department of Civil, Environmental and Natural Resources Engineering, Luleå University of Technology, Luleå, Sweden.
E-mail addresses: elaine_c.andrade@usp.br (E.C. Andrade), jeanlouzada@unifesspa.edu.br (J.C.G. Louzada), saeed.chelgani@ltu.se (S.C. Chelgani), lauleal@usp.br (L.S. Leal Filho).

https://doi.org/10.1016/j.jmrt.2024.10.245
Received 11 September 2024; Received in revised form 20 October 2024; Accepted 29 October 2024
Available online 30 October 2024

AP and AM macromolecules into the aqueous solution, characterized by the lack of debris (observed solely at SNMR of 7:1 and 9:1), coupled with greater availability of AP macromolecules in solution to depress hematite. In addition, starch prepared at SNMR = 5:1 released AP macromolecules to the solution with greater hydrodynamic diameter (d_H = 411 nm) than those released by the gelatinization conducted under SNMR = 3:1 (d_H = 353 nm). The recovery of hematite showed strong correlations ($r = -0.996$ and $R^2 = 0.99$) with the areas under the peaks related to the presence of AP in solution, indicating the higher availability of AP macromolecules to adsorb onto hematite/water interface [18].

While AP is recognized as the starch component that can act as a hematite depressant [5,18–23], the role played by AM in the system is poorly understood. In other words, the completeness of the starch gelatinization mechanism and its solubilization process through hematite depression have been not addressed. To fill these gaps, this study explored the rheological behavior of starch gels to reveal the completeness of the process associated with the effectiveness of hematite depression. Steady and dynamic shear rheological measurements and optical micrographs were used to assess gelatinization in various SNMRs.

2. Theoretical background

Native starch granules are insoluble in cold water due to their semicrystalline structure composed of concentric rings of alternating lamellae of amylose (AM) and amylopectin (AP) species. The amorphous regions are predominantly composed of AM species associated with a low content of large AP molecules, whereas short AP molecules comprise the crystalline lamellae [8,12,22,24–26]. To release its active matter (AP) into the solution, starch demands chemical or thermal gelatinization before its application in flotation systems. During the gelatinization process, starch granules swell until rupture, resulting in the leaching of AM plus AP species from the granules into the aqueous solution where AP molecules will interact with hematite particles and deactivate (depress) their surfaces [22,26–29]. The dissolution of starch granules is directly associated with its loss of birefringence and degree of crystallinity, which can be easily identified through optical microscopy (OM) with polarized light under crossed nicols. The total disappearance of typical structures known as “Maltese crosses” would be an indicator factor for the completeness of gelatinization [30–32].

2.1. DLVO theory

The prediction of starch performance to depress hematite can be approached by modeling the interaction of colloidal starch and hematite particles by DLVO theory [18,33]. This theory describes the magnitude and additivity of the short-range attractive Lifshitz-van der Waals (G^{LW}) and the long-range attractive/repulsive double-layer electrostatic (G^{EL}) interaction energies, as expressed in Eq. (1). The G^{LW} energy always decays strongly with the distance, while the G^{EL} energy can be either attractive or repulsive depending on the sign of the net interfacial electrical charge, acting in a long-range [34–36].

Additionally, the intensity of G^{LW} energy depends on a parameter known as the Hamaker constant (A), which governs the interaction between two (A_{131}, A_{232}) or three materials (A_{132}) in a heterogeneous system. This constant depends not only on the physical properties of the materials (phases involved) but also on their dielectric and refractive properties [34,35,37,38]. Consequently, G^{LW} energy varies depending on the type of system (e.g. for two infinite plates, for two spheres of radius a_1 and a_2, and sphere/plane plate interactions). As demonstrated by Rohem Peçanha et al. [33] and Andrade et al. [18], the A_{132} can be used to describe the attractive forces between a sphere (AP macromolecules) and a plane (hematite’s surface) (Eq. (2)). The A_{132} can be obtained from the individual Hamaker constants (A_{11}, A_{22} and A_{33}) for each phase involved (Eqs. (3) and (4)), since the indices 1, 2, and 3 are related to AP macromolecules, hematite particles, and water, respectively. Furthermore, the symmetrical Hamaker constants for starch (A_{131}) and hematite (A_{232}), both in aqueous medium, can be calculated using Eqs. (5) and (6), respectively [34,35,37,38].

$$G^{TOT} = G^{LW} + G^{EL} \tag{1}$$

$$G^{LW} = -\frac{A_{132}a}{6H} \tag{2}$$

$$A_{132} = \left(\sqrt{A_{11}} - \sqrt{A_{33}}\right)\cdot\left(\sqrt{A_{22}} - \sqrt{A_{33}}\right) \tag{3}$$

$$A_{132} = \sqrt{A_{131}}\cdot\sqrt{A_{232}} \tag{4}$$

$$A_{131} = \left(\sqrt{A_{11}} - \sqrt{A_{33}}\right)^2 \tag{5}$$

$$A_{232} = \left(\sqrt{A_{22}} - \sqrt{A_{33}}\right)^2 \tag{6}$$

Where variables are: G^{TOT}– total energy of interaction [J]; G^{LW}– Lifshitz-van der Waals energy of interaction [J]; G^{EL}– electrostatic energy of interaction [J]; a – radius of the colloidal starch particle [m]; H – the distance between starch particle (sphere) and hematite particle (planar surface) [m]; A_{132} – effective Hamaker constant between starch colloidal particles (index 1) and hematite particles (index 2) in aqueous medium (index 3) [J]; A_{131}– symmetrical Hamaker constant between starch colloidal particles (index 1) in aqueous medium (index 3) [J]; A_{232} – symmetrical Hamaker constant between hematite particles (index 2) in aqueous medium (index 3) [J]; A_{11}– individual Hamaker constant for starch colloidal particles in vacuum [J]; A_{22} – individual Hamaker constant for hematite particles in vacuum [J]; A_{33}– individual Hamaker constant for water molecules in a vacuum [J].

2.2. Rheological properties of starch gels

The rheological behavior of starch gels can be characterized by their viscoelastic and flow properties since several rheologic parameters can be obtained from state equations fitted to experimental curves: shear stress (τ) versus shear rate ($\dot{\gamma}$), apparent viscosity (η) versus shear rate ($\dot{\gamma}$), storage (G') and loss (G'') moduli versus angular frequency (ω), etc. [10,24,29,39–42]. There is a well-established relationship between averaged molecular weight (M_w) of a polymer and its zero-shear viscosity (η_0). The dependence of the η_0 on the M_w for linear and monodisperse polymers can be described by Eqs. (7) and (8). The critical molecular weight (M_c) is a point at which the molecular entanglements start happening, making the flow more difficult. This way, below M_c, polymeric molecules are not associated with others in aqueous medium. Accordingly, as $M_w > M_c$, Eq. (7) must be used, whereas $M_w < M_c$, Eq. (8) is more appropriate. In Eqs. (7) and (8), the constants K_1 and K_2 depend on the polymer type and temperature. The power law exponent (α) takes values varying between 3.2 and 3.9 [43–51]. Although starch is a biopolymer with bimodal size distribution due to the coexistence of AM and AP macromolecules, the parameter η_0 will undoubtedly provide an assessment of the magnitude of M_w, since Eqs. (7) and (8) reveal a direct proportionality between η_0 and M_w. Accordingly, polymers with a higher molar mass show higher values of η_0 [47,50].

$$\eta_0 = K_1.M_w^{\alpha} \tag{7}$$

$$\eta_0 = K_2.M_w \tag{8}$$

Under an applied external stress/strain, starch dispersions (gels) can exhibit simultaneous elastic (solid-like behavior) and viscous response (fluid-like behavior). Solid-like behavior is the consequence of a molecular network formed by a crosslinked matrix of coiled AM species, whereas fluid-like behavior is due to the presence of discrete AP colloidal species suspended in the aqueous medium [28,40]. One

behavior overrides another, depending on the AM content, its concentration in the solution [24,28,29,40], and the extent/type of the gelatinization process [28,29,40]. It was reported that the extent of the gelatinization process influences the hydrodynamic diameter (d_H) of the suspended AM (20 nm < d_H < 170 nm) and AP (100 nm < d_H < 1000 nm) colloidal particles, as well as debris from unreacted matter (3000 nm < d_H < 5600 nm) [18].

Small amplitude oscillatory shear (SAOS) tests have been widely used to determine the sol-gel transition point and to examine the fundamental viscoelastic properties of polymer/biopolymer samples [24,29,39,42,52–55]. SAOS tests are commonly performed in the linear viscoelastic range for each specific material, in which a strain (γ) or stress (τ) is applied in the form of a sinusoidal function with variable angular frequency (ω) and constant oscillatory amplitude (γ_0), measuring the resulting γ or τ [39,41,55–57]. The angular frequency (ω) is the number of oscillations per second, which is an indicator of the time scale of the experiment: short times correspond to high frequencies, whereas longer times are related to low frequencies. Frequency sweep (FS) tests provide information on the behavior and microstructure of gels, allowing us to assess whether they predominantly exhibit elastic or viscous properties, according to the profile of log-log curves where the G' (elastic component or storage modulus) plus G'' (viscous component or loss modulus) are plotted against the angular frequency (ω) adopted in the FS tests. For a viscoelastic gel (solid-like behavior), as a crosslinked polymer, the storage modulus is higher than the loss modulus ($G' > G''$). Conversely, for a viscoelastic gel (fluid-like behavior), as an uncrosslinked polymer, the loss modulus is higher than the storage modulus ($G'' > G'$). This way, the elastic component (G') is a measure of the energy stored by the gel during the test and subsequently released per cycle of deformation per unit volume. In addition, the viscous component (G'') indicates the amount of energy dissipated by internal friction when the gel flows. Before the accomplishment of any FS test, it is necessary to carry out previous strain sweep (SS) tests to ensure that the gel will be submitted to FS tests within its linear viscoelastic (LVE) region [8,29,39,43,55–57].

Another parameter commonly used to evaluate the rheological behavior of materials is the phase angle (δ), which is referred to as the loss tangent ($\tan\delta = G''/G'$). The latter is a function of the angular frequency (ω) and is directly related to energy lost per cycle (G'') divided by the energy stored per cycle of sinusoidal deformation (G'). As $\tan\delta < 1$, the elastic properties prevail over viscous ones, and for $\tan\delta > 1$, a weakened structure will be found, which reveals that the viscous character prevails over the elastic properties of the gel. Since $0° \leq \delta \leq 90°$, $\tan\delta$ can vary from zero to infinity. Thus, when $= 0°$ ($\tan\delta = 0$), the gel exhibits a purely elastic response, in which the maximum stress occurs at the maximum strain and both stress and strain are in the phase. Conversely, for an ideal viscous behavior, $= 90°$ ($\tan\delta \to \infty$), the stress and strain are completely out of the phase. Viscoelastic materials, such as starch gels, can exhibit both characteristics if elastic behavior prevails over viscous behavior ($G' > G''$), the phase angle lay in the range of $0° < \delta < 45°$. Conversely, if viscous behavior prevails over elastic behavior ($G'' > G'$), the phase angle varies in the range $45° < \delta < 90°$. The condition characterized by $G' = G''$ (or $\delta = 45°$) is called a sol-gel point because it represents the transition from fluid-like behavior to solid-like behavior during the gelatinization process [8,29,39,43,54–57].

For any viscoelastic material, such as starch gels, the linear stress response to a sinusoidal strain input is represented as the sum of the elastic components ($\gamma_0 G'$) of the stress in phase with the strain plus the viscous component ($\gamma_0 G''$) of the stress out-phased 90° with the applied strain, as shown in Eq. (9) [39,43,55–57].

$$\tau(t) = \gamma_0 G'(\omega)\sin\omega t + \gamma_0 G''(\omega)\cos\omega t \quad (9)$$

Where variables are: γ_0 – shear strain maximum [%]; G' and G'' – storage and loss moduli, respectively [Pa]; ω – angular frequency [rad/s]; t – time [s].

3. Materials and methods

3.1. Materials

Chunks of hematite from Carajás (Pará, Brazil) were provided from Vale SA. The sample was crushed to −1000μm, then dry ground to −150μm and deslimed by wet screening, yielding two products: flotation feed (−150 + 20 μm, d_{80} = 106 μm) and slimes (−20 μm). X-ray Fluorescence (XRF) and X-ray diffraction (XRD) analysis (Table 1) indicated that the sample was predominantly composed of hematite (97%), followed by magnetite (3%), and traces (<0.5%) of gibbsite, goethite, and quartz. Commercial purity of corn starch (Amidex™ 3001) was supplied by Ingredion – Brazil to act as a hematite depressant. Alkyl ether amine acetate (Flotigam® 7100) was supplied by Clariant – Brazil to act as a flotation collector. Iodine (I_2) and potassium iodide (KI) of analytical grade were provided by Neon Commercial Analytical Reagents LTDA – Brazil to prepare Lugol's solution used to identify AM/AP phases in the starch gels. Lugol's solution was prepared by dissolving 0.0165g I_2 and 0.0565g KI in 50 mL Milli-Q® water. NaOH)supplied by Labsynth-Brazil) was used to gelatinize starch and set pH. Milli-Q® water (resistivity = 18 MΩ cm) was used in the preparation of all starch gels, whereas distilled water (resistivity = 2 MΩ cm) was used for the flotation tests.

3.2. Preparation of starch gel

Starch gel solutions based on different SNMRs (Table 2) were prepared at a concentration of 6.5% (w/w) by mixing 2g of dry Amidex™ 3001 plus 29 mL of Milli-Q® water, followed by stirring for 10 min at room temperature. Different volumes of NaOH solution at 50% (w/w) were added to the starch suspension to achieve the desired SNMR and accomplish the gelatinization process. The suspension was stirred for 20 min at room temperature (23 ±1°C).

For all rheological measurements (both steady and dynamic shear tests), 6.5% (w/w) starch gels were used. For the flotation tests, 2% (w/w) stock solutions were prepared by diluting the original 6.5% (w/w) starch gel with Milli-Q® water, as illustrated in Fig. 1.

3.3. Flotation tests

Batch flotation tests were performed at room temperature (23 ±1°C) in a Dever sub-aerated cell (a 1.5 L stainless cell). The impeller speed was 1200 rpm with an airflow rate of 1.6L/min (gas holdup = 10%). For each test, the mineral suspension was prepared with a mass of 380 g of hematite and 700 mL of distilled water to obtain 35.2% (w/w) solids, and the pulp was stirred for 1 min. Thereafter, 175 μL of Amidex™ 3001 (prepared at SNMR of 3:1, 5:1, 7:1, 9:1) was added to the slurry and conditioned for 6 min at pH = 10.5. After depressant conditioning, 7 mL of Flotigam™ 7100 at 1% (w/w) was added and conditioned for a further 1 min. The air gauge was opened, and the flotation was carried out for 3 min. Floated and sink products were dried and weighed for hematite recovery (R) (Eq. (10)) and assessment of the degree of

Table 1
– Mineralogical and chemical composition of the flotation feed.

XRD (Rietveld analysis)	XRF analysis	
Minerals	Elements	Grade (%)
Hematite (97%)	Fe	68.90
Magnetite (3%)	SiO_2	0.87
Gibbsite (*)	Al_2O_3	0.24
Goethite (*)	P	0.01
Quartz (*)	Mn	0.04
	LOI(**)	0.35

(*)Traces (<0.5%).
(**)Loss on ignition.

Table 2
– Amount of NaOH for different SNMR.

SNMR	Volume of NaOH solution (*) [μL]	Moles of NaOH [x10^{-3}]
3:1	901	16.7
4:1	676	12.5
5:1	540	10.0
6:1	450	8.3
7:1	386	7.2
9:1	300	5.6

(*)Sodium hydroxide solution at 50% mass concentration.

hematite depression (D) (Eq. (11)).

$$R = \left(\frac{M_1}{M_1 + M_2}\right) \text{x } 100 \tag{10}$$

$$D = \left(\frac{R_i - R_a}{R_i}\right) \text{x } 100 \tag{11}$$

Where variables are: M_1 and M_2 – mass of the floated and sunk products, respectively. R_i and R_a – flotation recoveries of hematite without starch and in the presence of starch, respectively.

Each flotation test was conducted four times and the Statistica (version 14.0.0.15, supplied by TIBCO™ Software Inc.) was used for the data assessment. The results are reported as the mean ± standard deviation. The one-way analysis of variance (ANOVA) and Tukey's HSD multiple comparison tests at the significance level of $\alpha = 0.05$ were used to assess the statistically significant difference among the mean hematite recovery values (R). The degree of hematite depression (D) was calculated from the mean value of R and error propagation was assessed by the OriginPro™ software (version 2024, supplied by OriginLab Corporation, Northampton, MA, USA).

3.4. Optical microscopy

A drop of starch gels prepared at different SNMRs was placed on a glass plate and studied by transmitted light microscopy under parallel versus crossed nicols, at 22 ±1 °C (microscope Leica DMRXP equipped with MC190DH extended focus system camera). Starch gels were stained with Lugol's solution. The adopted mass ratios of iodine/amylose, iodine/amylopectin, and I_2/KI are in agreement with the literature, i.e., 17–22g I_2 per 100g AM, 1.05–1.25g I_2 per 100g AP and 29–37g I_2 per 100g KI, respectively [58,59].

3.5. Rheological measurements

Rheological measurements were conducted using a modular compact rheometer MCR 92 (Anton Paar GmbH, Austria), equipped with RheoCompass™ software. Rotational tests were used under controlled shear rate (CSR) mode, as well as oscillatory tests operating under controlled shear strain (CSD) mode. For this purpose, a concentric cylinder geometry was used (Mooney-Ewart type spindle). The diameters of the measuring bob (spindle) and cup were 26.66 and 28.92 mm, respectively. The gap length of measuring bob was 39.98 mm, the angle of the conical surface was 120° and the difference of radii corresponds to 1.13 mm. All rheological measurements were conducted using 6.5% (w/w) starch gels gelatinized with different SNMRs (3:1, 4:1, 5:1, 6:1, 7:1, and 9:1). For each SNMR, the starch gel was prepared twice according to section 3.2, and 18mL of the gel was transferred to the cup for rheological measurements at 22 ± 0.1 °C.

3.5.1. Steady shear flow tests

Measurements of shear stress (τ) versus shear rate ($\dot{\gamma}$), as well as apparent viscosity (η) versus shear rate ($\dot{\gamma}$) were conducted over the range of $0.1 \leq \dot{\gamma} \leq 100\ s^{-1}$. The results ($\tau$ x $\dot{\gamma}$) were fitted using the "Power Law" model (Eq. (12)), whereas the results (η x $\dot{\gamma}$) were fitted using the "Carreau-Yasuda" model (Eq. (13)) [60,61].

$$\tau = K(\dot{\gamma})^n \tag{12}$$

$$\eta = \eta_\infty + (\eta_0 - \eta_\infty) \cdot [1 + (\lambda.\dot{\gamma})^a]^{\frac{n-1}{a}} \tag{13}$$

Where variables are: τ – shear stress [Pa]; $\dot{\gamma}$ – shear rate [s^{-1}]; K – consistency coefficient [Pa.s^n]; n – power-law index [−]; η – dynamic viscosity [Pa.s]; η_0 and η_∞ – the zero-shear viscosity and the infinite-shear viscosity [Pa.s]; λ – relaxation time [s] where the critical shear rate ($\dot{\gamma} = 1/\lambda$) marks the onset of shear-thinning; a – width of the transition range between Newtonian and power law behavior [−]. For the general case, it holds $1 \leq a \leq 2$, however, for the Carreau model $a = 2$ [62].

3.5.2. Strain sweep tests

Strain sweep (SS) tests were performed with starch gels based on different SNMRs. The purpose of SS tests is to determine the maximum strain amplitude (γ_{max}) within the linear viscoelastic region (LVE). The magnitude of $\gamma_{max} = 10\%$ (Fig. 2) indicated that its value is insufficient

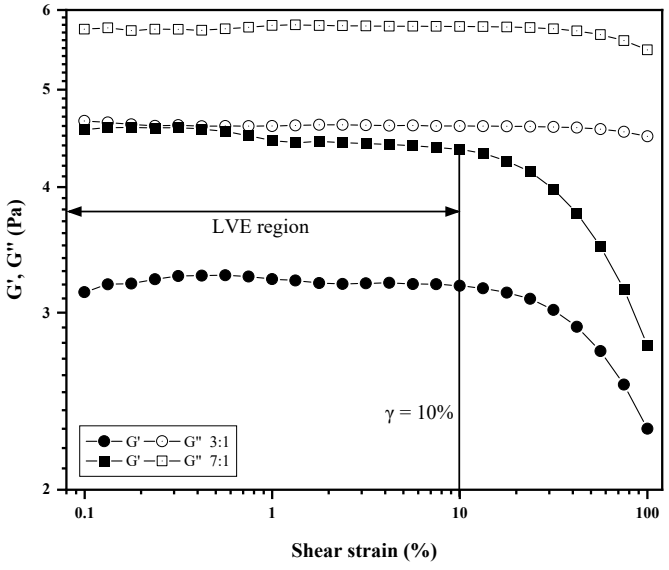

Fig. 2. – Amplitude sweeps for starch gels under SNMRs of 3:1 and 7:1.

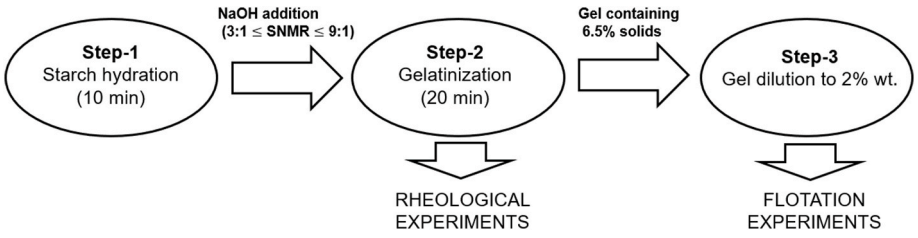

Fig. 1. – Schematic illustrating the preparation process of starch gel for rheological and flotation experiments.

to promote the structural breakdown of the starch gel for future FS tests. This way, its microstructural properties can be properly assessed.

3.5.3. Frequency sweep tests

Frequency sweep tests (FST) were carried out to evaluate the viscoelastic behavior of the starch gels for different SNMRs. They consist of dynamic oscillatory measurements conducted over a frequency sweep range of 0.1–10 (Hz) at 10% strain. The storage modulus (G') and loss modulus (G'') were plotted as a function of frequency (ω) in the log-log scale. The value of G' represents the stiffness of the gel strength and is related to the Young modulus. In addition, G'' indicates the deformation energy that is lost by internal friction (viscous dissipation) during shearing. As $G' > G''$, the sample exhibits a solid (or solid-like) structure. Conversely, the sample behaves as viscoelastic fluid whenever $G'' > G'$. The experimental results (G', G'' x ω) were fitted using the "Power Law" models (Eqs. (14) and (15)). Additionally, the parameter tan δ, another output of the FST test, was evaluated as a function of frequency.

$$G' = K'(\omega)^{n'} \tag{14}$$

$$G'' = K''(\omega)^{n''} \tag{15}$$

Where variables are: G', G''– storage and loss moduli [Pa]; ω – angular frequency [Hz]; K', K''– intercepts [−]; n', n''– slopes [−].

4. Results and discussion

4.1. Flotation

Flotation results (Fig. 3) for various SNMR and NaOH moles indicated that in the absence of starch (0 mg/L) and the presence of collector (100 mg/L of Flotigam®7100), hematite recovery was 35.3%. This high hematite floatability would be translated to the need for a depressant to promote the separation selectivity between quartz and hematite through the quartz reverse cationic flotation [1,3,20,63,64]. However, by adding starch, the hematite floatability decreased (hematite depressed). Hematite depression increased by changing the SNMR from 9:1 to 7:1 and then 5:1. Flotation outcomes showed that the minimum hematite recovery ($R = 14.8\%$) (corresponds to the maximum hematite depression) occurred when SNMR was 5:1 (corresponds to $1x10^{-2}$ mol of NaOH added to the gelatinization process). The SNMR = 9:1 yielded the highest hematite recovery ($R = 29.1\%$) in the presence of the depressant, highlighting the low depressant efficiency in this Starch:NaOH ratio due to the incomplete gelatinization [18]. Optical microscopy and rheological studies were conducted to correlate the interactions within starch gelatinization and its hematite depression efficiency.

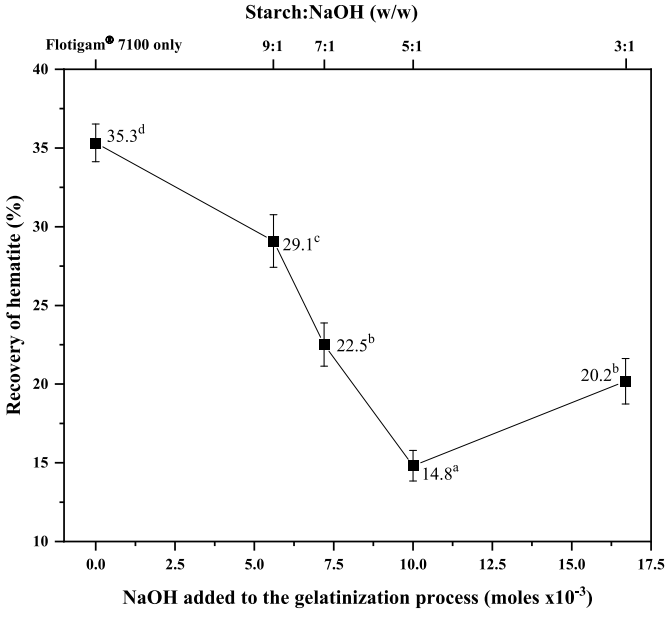

Fig. 3. – Recovery of hematite as a function of NaOH moles at pH 10.5. Averaged values accompanied by different letters are significantly different ($p < 0.05$).

4.2. Optical microscopy

To highlight the correlation between the depressant preparation by starch:NaOH ratio, SNMRs for the highest and lowest hematite recovery were considered for the optical microscopy (SNMR = 9:1 vs. 5:1) (Fig. 3). Micrographs taken from starch gels prepared with SNMR = 5:1 versus SNMR = 9:1 after the accomplishment of the gelatinization process is depicted in Fig. 4. Micrographs related to observations conducted under parallel nicols indicated that gelatinization prepared with SNMR = 5:1 yielded a smooth and homogeneous matrix displayed (Fig. 4a). However, a heterogeneous mixture related to SNMR = 9:1 demonstrated (Fig. 4b) an incomplete gelatinization process with the occurrence of large granules (diameter up to 20,000 nm). The large granules related to SNMR = 9:1 exhibited the typical Maltese Cross profile (Fig. 4d), indicating the pristine semi-crystalline structure preserved by non-gelatinized starch granules. On the other hand, Fig. 4c shows a dark background, corroborating the homogenous matrix yielded by the gelatinization process carried out with SNMR = 5:1.

Since the reactions between iodine and starch components (AM, AP) yield complexes typically exhibiting either blue (iodine-AM) or purple (iodine-AP) colors [58,65], staining caused by those reactions can be used to characterize the distribution of AM and AP phases in starch gels prepared with SNMR = 5:1 versus 9:1. The large granules (Fig. 4f) related to non-gelatinized starch (SNMR = 9:1) are entrapping AP species. They contrasted with a background matrix composed of abundant blue color complexes addressed to the dominance of AM species. AM species are promptly leached from the granules in the early stages of the gelatinization process, regardless of the SNMR used in the system. The gelatinization conducted with SNMR = 5:1 (Fig. 4e) indicated a complete disintegration of pristine starch granules liberating both AM and AP species to the solution, where AP species are evenly distributed in the system [65,66]. It was also reported that since AP molecules (and not AM species) are responsible for hematite depression [5,19–23], greater availability of AP species in gels prepared with SNMR = 5:1 versus SNMR = 9:1 endorsed the most efficient hematite depression (Fig. 3).

4.3. Rheological properties

4.3.1. Flow behavior

Shear stress (τ) versus shear rate ($\dot{\gamma}$), and apparent viscosity (η) versus shear rate ($\dot{\gamma}$) obtained from starch gels containing 6.5% (w/w) of solids and conditioned with different SNMR (3:1, 4:1, 5:1, 6:1, 7:1 and 9:1) are depicted in Fig. 5a and b, respectively. These results revealed a shear-thinning behavior for all starch gels since all of them flow more definitely while the shear rate increased. Similar trends were reported in other investigations while the starch gels containing up to 30% (w/w) of solids [28,67–72]. Experimental results also indicated (Fig. 5a) that the Power Law model (Eq. (12)) fitted the provided points ($R^2 \geq 0.997$), which is considered the simplest model to describe the rheological behavior of non-Newtonian fluids at moderate shear rates [61,73,74]. The model outcomes (Table 3) showed that as SNMR increased from 3:1 to 9:1, the consistency index (K) increased from 1.03 to 7.57 Pa.s^n, whereas the fluid behavior index (n) decreased from 0.79 to 0.50. Regardless of the SNMR, as n is below 1, the yielded gels could be classified as pseudoplastic (shear-thinning) fluids, since the gel becomes less resistant to flow as the shear rate increases.

Starch degradation during the gelatinization process can also provide insights to better understand the rheological behavior of gels

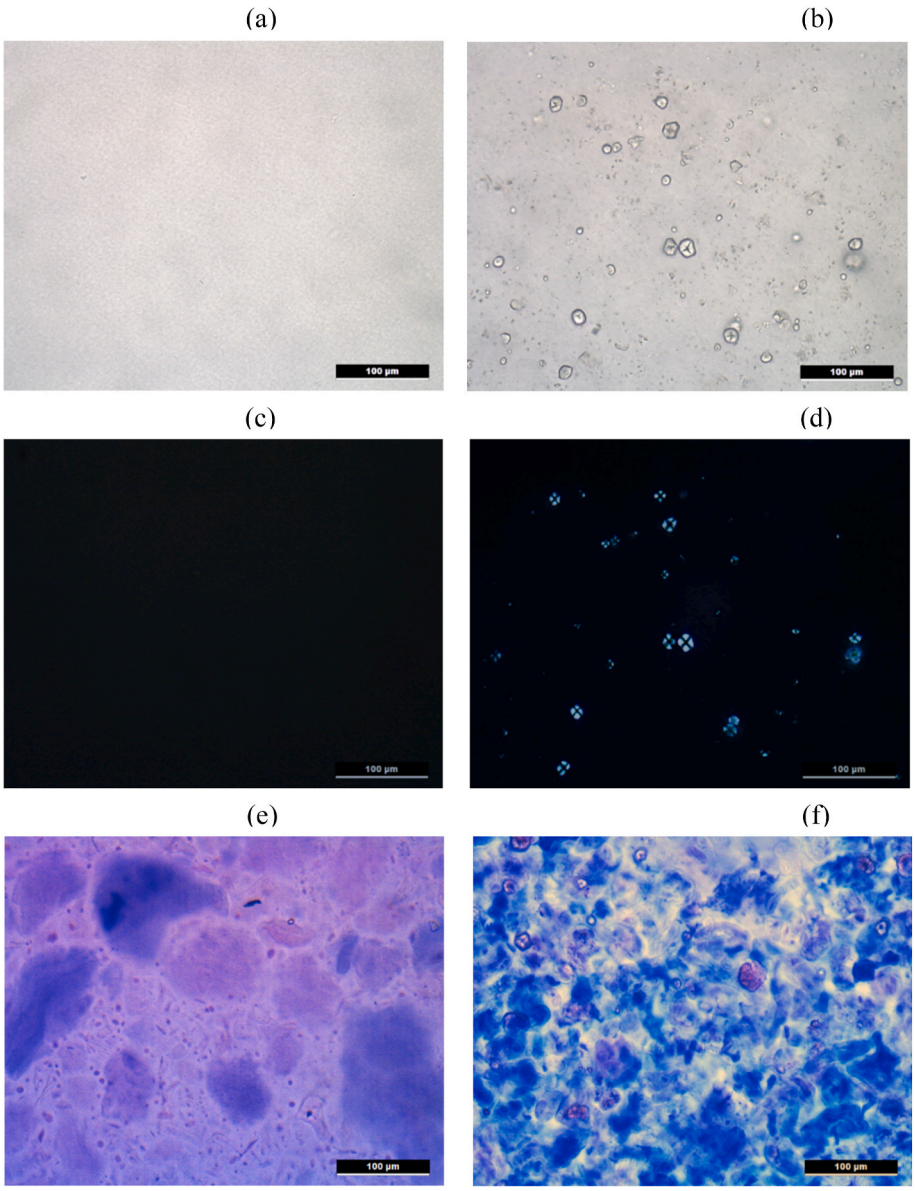

Fig. 4. – OM micrographs at 200× magnification of starch gels prepared in different SNMRs under parallel versus crossed nicols and iodine staining from top to bottom: (a), (c) and (e) for SNMR = 5:1; and (b), (d) and (f) for SNMR = 9:1.

prepared with different SNMRs. Andrade et al. [18] indicated that AM degradation due to excessive NaOH added to the gelatinization process. The hydrodynamic diameter (d_H) of AM molecules in aqueous gels decreased from 98 (SNMR = 9:1) to 54 nm (SNMR = 3:1) [18]. Considering that more alkaline solutions promote starch decomposition [22,75,76], gels prepared with lower SNMR (3:1) would show less effective entanglements between AM coiled chains than gels prepared with higher SNMR (9:1). Those entanglements can be considered the cause for a higher resistance posed by the gel to shear flow [46,71,77]. Such a behavior could be reflected in the magnitude of the parameter K (consistency index) (Table 3), which increased as the SNMR increased from 3:1 to 9:1. In addition, the n magnitude decreased as the SNMR increased from 3:1 to 9:1, which showed the gels exhibit an increasingly pseudoplastic (shear-thinning) behavior.

Moreover, experimental results (Fig. 5b) indicated that plotted points (η x $\dot{\gamma}$) were fitted very well (R^2 = 1.00) in the Carreau-Yasuda model (Eq. (13)) (Table 3). These parameters (zero-shear viscosity (η_0), infinite-shear viscosity (η_∞), relaxation time (λ), and critical shear rate ($\dot{\gamma}_{crit}$)) are useful to reveal the structural properties and flow behavior of starch gels gelatinized with different SNMR. The value of η_0 increased continually when the NaOH in the gelatinization process was decreased, indicating starch degradation increased as SNMR decreased from 9:1 to 3:1. It was well understood that the rationale provided by Eqs. (7) and (8) show a direct proportionality between η_0 and polymer molar mass (M_w): polymers with higher molar mass will show higher values of η_0 [43–51]. Values of η_0 displayed in Table 3 can be ordered in the following SNMR sequential order: 9:1 (η_0 = 84.8 Pa s) > 7:1(η_0 = 32.0 Pa s) > 6:1(η_0 = 2.7 Pa s) > 5:1(η_0 = 2.4 Pa s) > 4:1(η_0 = 1.9 Pa s) > 3:1(η_0 = 1.8 Pa s). Since high values of η_0 ± errors are associated with the elastic-solid behavior [48], it is possible to probe that starch gels exhibited the highest values when SNMR was higher (7:1 and 9:1). The abrupt increase in η_0 for SNMRs = 7:1 and 9:1 can be attributed to incomplete gelatinization, as the presence of debris was observed in these starch dispersions (Fig. 4b and f), consistent with the findings of Andrade et al. [18]. This suggests a more pronounced solid-viscoelastic behavior compared to those prepared with lower SNMRs (6:1, 5:1, 4:1 and 3:1), as will be discussed in section 4.3.2. Unlike η_0, η_∞ does not provide information on polymer molecular weight, because it is

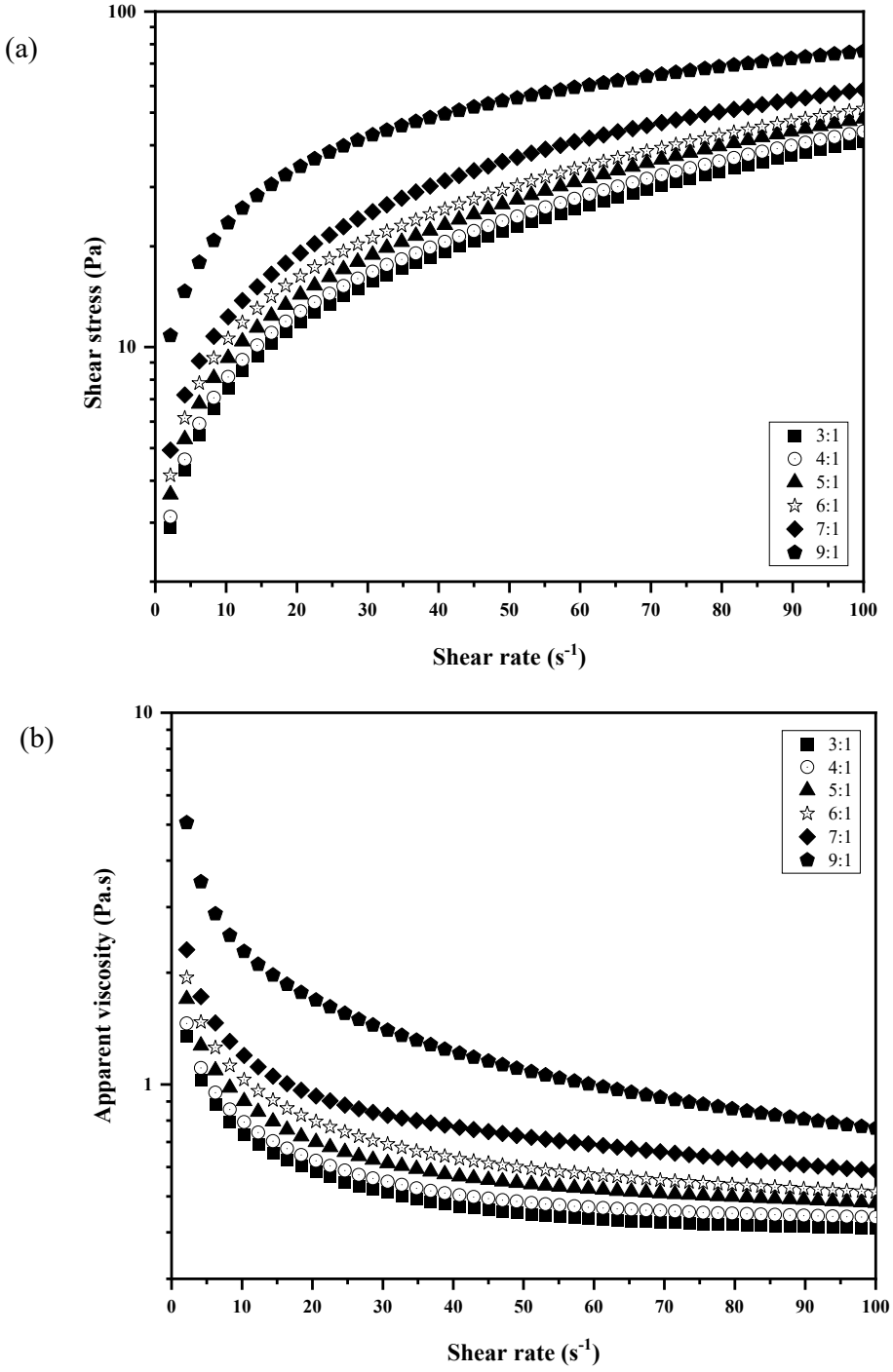

Fig. 5. – Steady flow curves for corn starch gels at 6.5% (w/w) gelatinized in different SNMRs: (a) shear stress versus shear rate and (b) apparent viscosity versus shear rate.

determined at shear rates ($\dot{\gamma} \geq 10^3 s^{-1}$), in which the fluid has already reached its minimum flow resistance [48,49,52].

4.3.2. Viscoelastic properties

The mechanical spectra ($0.1 \leq \omega \leq 10$Hz) of starch gels containing 6.5% solids w/w and gelatinized with different SNMR are shown in Fig. 6. Curves related to the elastic (G') and viscous (G'') components versus ω were fitted by the Power Law model ($R^2 \geq 0.992$) and its intercept-values (K', K'') as well as slopes-values (n', n'') are shown in Table 4. For gels prepared with 3:1 $\leq$ SNMR $\leq$ 5:1, the viscous component was always higher than the elastic component ($G'' > G'$), revealing a fluid-viscoelastic behavior within the explored frequency range. Conversely, for gels prepared with SNMR $\geq$ 7:1, G' prevailed over G'' ($G' > G''$), characterizing a solid-viscoelastic behavior. In addition, the SNMR = 6:1 showed an overlap of the G' and G'' ($G' \approx G''$), revealing a transition point from liquid-like to solid-like behaviors. These results are in agreement with the parameter tan δ, which is the ratio between the dissipated (G'') and stored (G') energies [29,39,55,78,79]. Plots of tan δ versus ω for gels prepared with 3:1 $\leq$ SNMR $\leq$ 9:1 (Fig. 6) indicated that for the SNMR range between 3:1 to 5:1, the mean values of tan δ were greater than one ($1.2 \leq$ tan $\delta \leq 1.4$), meaning the predominance of viscous properties were over elastic properties. On the other hand, for

Table 3
– Fit parameters ±standard errors of the Carreau-Yasuda and Power Law models for aqueous starch dispersions gelatinized with different SNMRs.

SNMR	Carreau-Yasuda (*)					Power Law		
	η_0 [Pa.s]	η_∞ [Pa.s]	λ [s]	$\dot{\gamma}_{crit}$ (**) [s^{-1}]	R^2	K [Pa.s^n]	n [−]	R^2
3:1	1.82 ± 0.07	0.30 ± 0.01	0.69 ± 0.08	1.46 ± 0.16	1.00	1.03 ± 0.04	0.79 ± 0.01	0.99
4:1	1.95 ± 0.07	0.33 ± 0.01	0.66 ± 0.07	1.52 ± 0.16	1.00	1.11 ± 0.04	0.79 ± 0.01	0.99
5:1	2.37 ± 0.08	0.35 ± 0.01	0.74 ± 0.08	1.35 ± 0.12	1.00	1.35 ± 0.04	0.77 ± 0.01	0.99
6:1	2.69 ± 0.06	0.33 ± 0.01	0.77 ± 0.05	1.30 ± 0.09	1.00	1.76 ± 0.05	0.73 ± 0.01	0.99
7:1	31.98 ± 12.14E+3	0.34 ± 0.01	94.34 ± 69.13E+3	0.01 ± 7.77	1.00	2.34 ± 0.03	0.70 ± 0.00	0.99
9:1	84.83 ± 10.44E+4	0.02 ± 0.04	167.10 ± 424.24E+3	0.01 ± 15.19	1.00	7.57 ± 0.08	0.50 ± 0.00	0.99

(*)The interaction algorithm used was Orthogonal Distance Regression with a maximum interaction performed = 315. The parameter a was set to a value of 2 and parameter n was not shown due to its low accuracy.
(**)For $\dot{\gamma}_{crit}$, the standard error was estimated using the Propagation of Error App in OriginPro™ software.

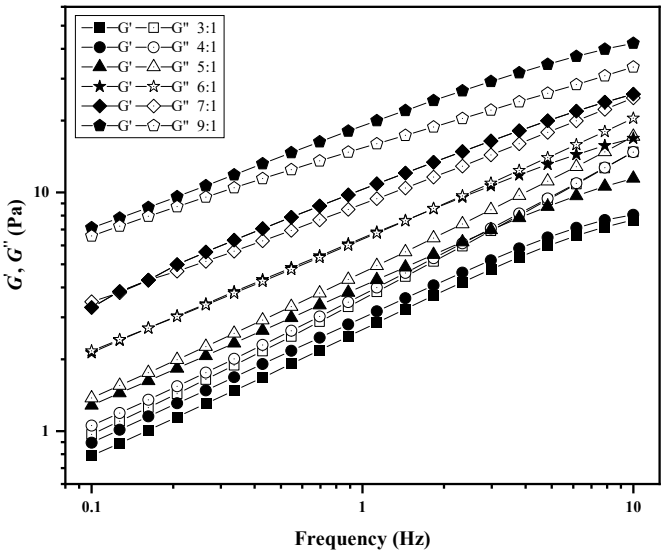

Fig. 6. – Dynamic frequency sweep data for starch gels at 6.5% (w/w) gelatinized in different SNMRs. Each condition was tested two times and a mean curve was obtained.

Table 4
– Fit parameters ±standard errors of the Power Law model for the G' and G'' curves and mean values for tan δ of the starch dispersions gelatinized under different SNMRs.

SNMR	G' (Storage modulus)			G'' (Loss modulus)			tan $\delta = G''/G'$ [−]
	K' [Pa.s^n]	n' [−]	R^2	K'' [Pa.s^n]	n'' [−]	R^2	
3:1	2.70 ± 0.05	0.48 ± 0.01	0.99	3.57 ± 0.02	0.61 ± 0.00	0.99	1.41 ± 0.19
4:1	3.00 ± 0.06	0.46 ± 0.01	0.99	3.73 ± 0.02	0.59 ± 0.00	0.99	1.32 ± 0.18
5:1	4.07 ± 0.05	0.47 ± 0.01	0.99	4.62 ± 0.03	0.56 ± 0.00	0.99	1.18 ± 0.12
6:1	6.43 ± 0.07	0.44 ± 0.01	0.99	6.40 ± 0.03	0.50 ± 0.00	0.99	1.03 ± 0.06
7:1	10.18 ± 0.10	0.42 ± 0.01	0.99	9.01 ± 0.04	0.44 ± 0.00	0.99	0.91 ± 0.05
9:1	18.71 ± 0.23	0.37 ± 0.01	0.99	15.20 ± 0.04	0.34 ± 0.00	0.99	0.83 ± 0.06

7:1 ≤ SNMR ≤ 9:1 the mean values of tan δ were lower than 1 (0.8 ≤ tan δ ≤ 0.9) pointing out that the predominance of elastic properties was over viscous properties. Additionally, the gel prepared with SNMR = 6:1 showed a fair balance ($G' \approx G''$, tan $\delta = 1.0$) between elastic and viscous properties.

Based on these outcomes (Table 4), gels prepared with 3:1 ≤ SNMR ≤ 5:1 exhibited $K'' > K'$ (the viscous character prevails over the elastic character), indicating that starch gels revealed a predominant fluid-like behavior properly associated with a higher complete dissolution of starch grains (as illustrated by Fig. 4a and e). Conversely, since gels prepared with 6:1 ≤ SNMR ≤ 9:1 exhibited $K' > K''$ (the elastic character prevails over the viscous character), signalizing an incomplete dissolution of starch granules (Fig. 4b and f). It has to be noticed that for SNMR = 6:1, K' (6.43 Pa.s^n) was slightly higher than K'' (6.40 Pa.s^n), which indicated the onset of solid-viscoelastic behavior (Figs. 6 and 7). In Table 4, the slopes n' and n'' are related to the gel's oscillating shear behavior, in which values of n' and n'' greater than zero indicated a dependency of G' and G'' with the frequency (ω), while those values are very close or equal to zero, indicating that G' and G'' are independent of the applied frequencies. In addition, the value of the slope n' showed whether a gel was sufficiently strong to be independent of the applied frequency (n' tending to zero), such as those gels that exhibited a three-dimensional crosslinked molecular network. Contrarily, greater values of n' characterize weak gels, whose G' and G'' depend on the applied frequency [39,41,72,80]. Model outcomes also demonstrated (Fig. 6) that curves $G'(\omega)$ and $G''(\omega)$ related to gels prepared under different

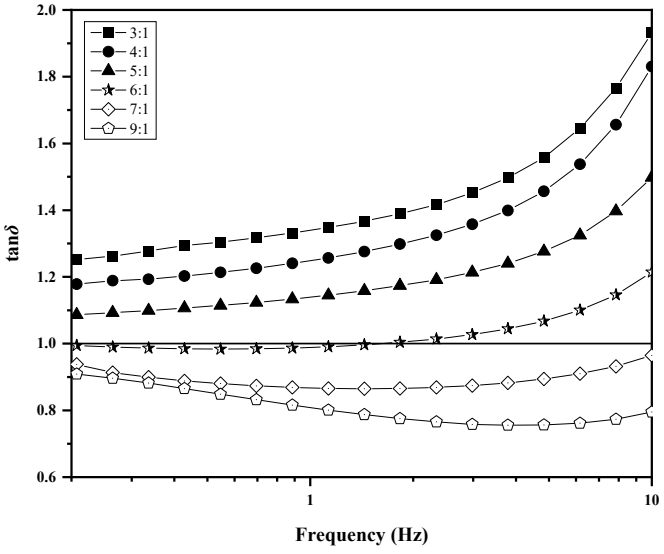

Fig. 7. – Loss tangent (tan δ) as a function of frequency for starch gels at 6.5% (w/w) gelatinized in different SNMRs.

SNMR (from 3:1 to 9:1) had a high dependence on frequency within the range 0.1–10 Hz since $0.4 \leq n' \leq 0.5$ and $0.3 \leq n'' \leq 0.6$. This type of spectrum was linked to weak gels even for the conditions in which $G' > G''$ (SNMR = 7:1 and 9:1), because n' equals 0.4 ($n' = 0.4$), as displayed in Table 4.

Moreover, modeling outcomes (Table 4) indicated that the magnitude of η_∞ is probably influenced only by the intensity of the fluid pseudoplastic behavior, since the parameter n (from the Power Law model) and also η_∞ (from Carreau-Yasuda model) were practically constant in the range from SNMR = 3:1 ($n = 0.8$, $\eta_\infty = 0.3$ Pa s) to SNMR = 7:1 ($n = 0.7$, $\eta_\infty = 0.3$ Pa s), but they decreased abruptly at SNMR = 9:1 ($n = 0.5$, $\eta_\infty = 0.02$ Pa s). After the cessation of an external strain/stress applied to a gel, the time taken by viscoelastic materials to reach the steady state at the molecular level is known as relaxation time (λ). This way, low values of λ are related to fluid-like behavior, whereas higher values of λ are addressed to solid-like behavior [43,52,55]. Regarding the experimental results displayed in Table 3, the lowest values of relaxation time ($\lambda \leq 0.8$s) observed for 3:1 ≤ SNMR ≤ 6:1 indicated that those starch gels exhibit a predominant fluid-like behavior. Conversely, starch gels prepared with SNMR = 7:1 (λ = 94.3s) and 9:1 (λ = 167.1s) show a predominantly solid-like behavior. On the other hand, the transition from Newtonian to pseudoplastic behavior is marked by the critical shear rate ($\dot{\gamma}_{crit}$). According to values displayed in Table, 3, gels prepared with SNMR ≥ 7:1 show pseudoplastic behavior even under very low shear rates ($0.01 s^{-1}$), whereas gels prepared with SNMR<7:1 exhibit $\dot{\gamma}_{crit}$ varying from 1.3 to 1.5 s^{-1}. This trend is corroborated by the magnitude of the parameter n of the Power Law model, approached before in this section.

4.4. Micro and macro variables

Outcomes of rheological experiments (Figs. 6 and 7) indirectly showed that the amount of NaOH added to the gelatinization process greatly influenced the viscoelastic properties of starch gels. It was well understood that the alkalinity of aqueous solutions plus dissolved oxygen promotes oxidative reactions, can decompose starch [22,28,71,75,76], and eventually, influencing its interaction with hematite [81,82]. Since the amount of NaOH added to the gelatinization process increased (the SNMR decreased), it would be expected that starch decomposition was more intensive as the gelatinization process was accomplished with lower values of SNMRs.

As mentioned (section 4.3.1), the parameter zero-shear viscosity (η_0) represents the weighted arithmetic mean of the molecular weight ($\overline{M_w}$) of a polymer and it decreases with the alkalinity of the system. This behavior showed a correlation (Fig. 8) between starch rheology parameters and its depression effect, where η_0 strictly decreased with the amount of NaOH added to the gelatinization process. This trend was corroborated by the values of d_{AM} (Table 5) related to starch gels prepared in the range 3:1 ≤ SNMR ≤ 9:1. To account for the interactions between starch colloidal particles (index 1) suspended in the aqueous medium (index 3), Andrade et al. [18] also determined the magnitude of the Hamaker constant (A_{131}) related to gels prepared with different SNMRs. They indicated that the Hamaker constant of the starch/water/hematite system (2.9×10^{-20} J < A_{132} < 3.3×10^{-20} J).

Modeling results (Table 5) also showed that A_{131} increased with SNMR, which eventually influenced the rheological behavior (tan δ) of the starch gels. Based on Eq. (16), the independent variables d_{AM}, d_{AP}, and A_{131} were strongly correlated (Table 6) to the rheological behavior (tan δ) of the starch gels approached. The results of the multiple regression analysis (Table 6) indicated that the model has statistical significance since the F-test (ANOVA) presents a p-value smaller than 0.05 ($p < 0.001$). Thus, the null hypothesis (H_0) was rejected, and the alternative hypothesis (H_1) was accepted in which at least one of the coefficients was not zero. Additionally, a high coefficient of determination ($R^2 = 0.947$) was obtained, indicating that the independent micro variables (d_{AM}, d_{AP}, and A_{131}) could explain 94.7% of the variation in the value of tan δ (macro variable). Accounting for the magnitude of the standardized regression coefficients, the coefficient of micro variable d_{AM} shows by far the highest absolute value, |-0.71|, followed by the coefficients related to the A_{131} and d_{AP} variables with values of 0.53 and 0.45, respectively, suggesting that d_{AM} is the most important of the three independent variables. Thus, the major influence exerted by the hydrodynamic diameter of AM species (d_{AM}) on the rheological behavior of starch gels (tan δ) was probably due to its effective self-entanglement in

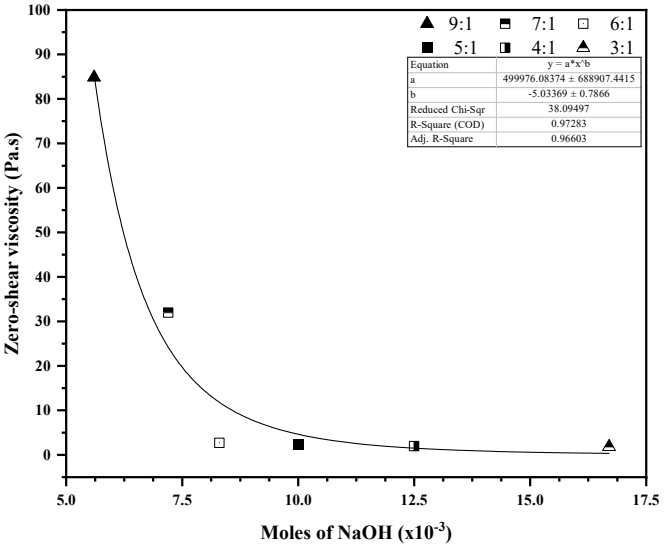

Fig. 8. – Zero-shear viscosity versus moles of NaOH added to the gelatinization process.

Table 5
– The influence of the amount of NaOH added to the gelatinization process on the hydrodynamic diameter of AM (d_{AM}) and AP (d_{AP}) molecules, Hamaker constant of starch-starch molecular interactions in aqueous medium (A_{131}), and gel rheology (tan δ).

Moles of NaOH [x10^{-3}]	SNMR	d_{AM} (*) [x10^{-8}m]	d_{AP} (*) [x10^{-8}m]	A_{131} (*) [x10^{-21}J]	tan $\delta = G''/G'$ [–]
16.7	3:1	5.4 ± 0.1	35.3 ± 0.6	11.4 ± 0.3	1.4 ± 0.2
10.0	5:1	7.5 ± 0.1	41.1 ± 0.1	9.2 ± 0.1	1.2 ± 0.1
7.2	7:1	8.5 ± 0.6	38.0 ± 0.6	9.0 ± 0.3	0.9 ± 0.1

(*)Andrade et al. [18].

Table 6
– Multiple regression summary for the dependent variable tan δ versus independent variables d_{AM}(*), d_{AP}(*) and A_{131}(*).

Variables	Standardized coefficients	Standard errors	t-values	p-values	Multiple correlation coefficient (R) (**)
Intercept = −0.45	–	–	−0.26	0.81	–
d_{AM}	−0.71	0.39	−1.83	0.13	−0.94
d_{AP}	0.45	0.19	2.33	0.07	−0.40
A_{131}	0.53	0.48	1.11	0.32	0.86
tan δ	–	–	–	–	1.00

(*)N = 9, $R = 0.97332781$, $R^2 = 0.94736702$, Adjusted $R^2 = 0.91578724$; F-test: $F(3,5) = 29.999$, $p < 0.00127$, standard error of estimate = 0.06232, where N = 9 refers to the number of samples used for the statistical test, specifically three average values for d_{AM}, d_{AP}, and A_{131}.
(**)Relative to tan δ versus any independent variable.

solution, making starch gels more elastic and stronger [71,83,84].

$$\tan\delta = G''/G' = -0.45 - 0.71d_{AM} + 0.45d_{AP} + 0.53A_{131} \quad (16)$$

Gao et al. [85] reported that increasing amounts of NaOH added to the gelatinization process could decrease the entanglement and strength of starch gels by weakening van der Waals forces and breaking hydrogen bonds between molecules. Consequently, based on the modeling outcomes (Table 3: consistency index, K, and Table 4: tan δ or K', K'' intercepts) as the amount of NaOH added to the gelatinization process increased from $5.6x10^{-3}$ mol (SNMR = 9:1) to $1.7x10^{-2}$ mol (SNMR = 3:1), starch gels offered less resistance to flow (ever-decreasing values of K) and became more viscous and less elastic, since values of K'' tend to be higher than K' and tan $\delta > 1$.

4.5. Rheology versus gelatinization

Starch gels prepared with SNMR<6:1 exhibited a homogeneous and smooth matrix (Fig. 4a and e). They also showed tan $\delta > 1$, as well as the lowest values of relaxation times ($\lambda \leq 0.7$s) plus zero-shear viscosities ($\eta_0 \leq 2.4$ Pa.s). All those characteristics highlighted a complete gelatinization process, cast by a dominant fluid-like behavior. Conversely, as SNMR>6:1, starch gels showed a heterogenous matrix formed by evident non-gelatinized matter (starch granules) (Fig. 4d and f), in which AP species are entrapped within the granules and AM molecules are released to the solution. Those gels also indicated tan $\delta < 1$, as well as the highest values of relaxation times ($\lambda \geq 94.3$ s) plus zero-shear viscosities ($\eta_0 \geq 32.0$ Pa s), casting a prevailing solid-like behavior. As the gelatinization process was carried out with SNMR = 6:1, the yielded gel tended to exhibit a fair balance between fluid-like versus solid-like behavior, since tan $\delta = 1$.

Analyzing the data also showed (Fig. 9), the fluid-like behavior (tan $\delta > 1$) exhibited by the starch gels prepared with SNMR<6:1, promoted the highest degree of hematite depression at SNMR = 5:1 (58% of depression). The complete gelatinization (SNMR<6:1) certainly assisted in dissolving the starch pristine granules and released AP species to the aqueous solution to depress hematite. However, Andrade et al. [18] documented that the most effective depression (SNMR = 5:1) was attained as the Lifshitz-van der Waals component (G^{LW}) of the free energy of interaction between hematite particles and AP nano molecules was higher for SNMR = 5:1 compared to SNMR = 3:1. Accordingly, a compromise between AP molecular size (d_{AP}) and the effective Hamaker constant (A_{132}) of the interaction between starch (index 1) and hematite (index 2) immersed in the aqueous medium (index 3) found with SNMR = 5:1 offer better conditions to depress hematite than SNMR = 3:1, in spite both gels exhibit a fluid-like behavior. Self-entanglement of bigger and easily released AM molecules from the starch granules, when there was a lack of NaOH in the gelatinization process, provoked the solid-like gel behavior which demonstrated incomplete gelatinization and poor hematite depression.

5. Conclusion

The rheological behavior of starch gels prepared under a wide range of SNMR (3:1 ≤ SNMR ≤ 9:1) had been used to identify the completeness of the gelatinization process, to understand the role played by AM and AP species in the system, and to improve the knowledge on starch preparation to maximize hematite depression through the cationic reverse flotation aiming at concentrating iron ore. Investigation outcomes highlighted deeper analyses such as FTIR and SEM can enhance the rheology studies which indicated:

- Starch gels exhibited shear-thinning behavior (n < 1) across SNMR values between 3:1 and 9:1, becoming less resistant to flow as the shear rate increased. As the SNMR increased from 3:1 to 9:1, stronger and more pseudoplastic gels were formed, since a continuous reduction in NaOH resulted in incomplete gelatinization with the presence of debris at higher SNMRs (7:1 and 9:1), causing solid-viscoelastic behavior to prevail over liquid-viscoelastic behavior.
- Gels with SNMR >6:1 showed solid-like behavior due to excess amylose (AM), while SNMR ≤5:1 resulted in liquid-like behavior, influenced by higher alkalinity and reduced AM macromolecule size.
- A model linking rheological behavior to molecular variables showed that AM size (d_{AM}) had the greatest impact, followed by the Hamaker constant (A_{131}) and AP size (d_{AP}).
- The most effective hematite depression was achieved at SNMR = 5:1 and not SNMR = 3:1, since the excessive decrease of d_{AP} by NaOH yielded by SNMR = 3:1 reduces the magnitude of the Lifshitz-van der Waals interaction energy (G^{LW}) between AP molecules and hematite surface. Conversely, SNMR = 5:1 offers a better combination of AP molecular size (d_{AP}) and the effective Hamaker constant (A_{132}) which favors hematite depression, despite both gels exhibiting a fluid-like behavior.

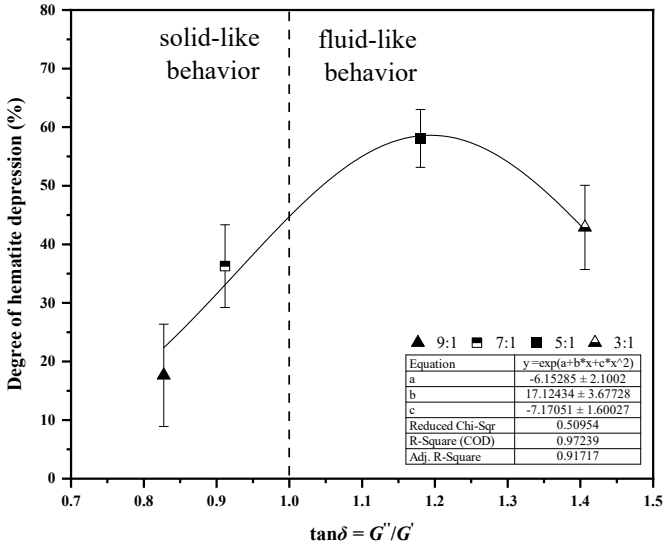

Fig. 9. – Degree of hematite depression versus tan δ for starch gels containing 6.5% of solids (w/w) and gelatinized with different SNMRs (The error bars represent estimated error for a 95% confidence interval).

Author contribution

Elaine Cristina Andrade: Writing – original draft, Methodology, Investigation, Formal analysis, Data curation, Conceptualization. Jean Carlo Grijó Louzada: Writing – review & editing, Conceptualization. Saeed Chehreh Chelgani: Writing – review & editing, Writing – original draft, Visualization, Validation, Methodology, Investigation, Formal analysis, Conceptualization. Laurindo de Salles Leal Filho: Supervision, Writing – review & editing, Writing – original draft, Visualization, Validation, Methodology, Investigation, Formal analysis, Conceptualization.

Declaration of interests

The authors declare that they have no known competing financial interests or personal relationships that could have appeared to influence the work reported in this paper.

Acknowledgments

The authors express their gratitude to Vale S.A. for providing the hematite sample and CAPES for providing a scholarship to one of the authors.

References

[1] Kar B, Sahoo H, Rath SS, Das B. Investigations on different starches as depressants for iron ore flotation. Miner Eng 2013;49:1–6. https://doi.org/10.1016/j.mineng.2013.05.004.

[2] Nykänen VPS, Braga AS, Pinto TCS, Matai PHLS, Lima NP, Leal Filho LS, et al. True flotation versus entrainment in reverse cationic flotation for the concentration of iron ore at industrial scale. Miner Process Extr Metall Rev 2020;41:11–21. https://doi.org/10.1080/08827508.2018.1514298.

[3] Shrimali K, Atluri V, Wang Y, Bacchuwar S, Wang X, Miller JD. The nature of hematite depression with corn starch in the reverse flotation of iron ore. J Colloid Interface Sci 2018;524:337–49. https://doi.org/10.1016/j.jcis.2018.04.002.

[4] Shrimali K, Jin J, Hassas BV, Wang X, Miller JD. The surface state of hematite and its wetting characteristics. J Colloid Interface Sci 2016;477:16–24. https://doi.org/10.1016/j.jcis.2016.05.030.

[5] Yang S, Wang L. Structural and functional insights into starches as depressant for hematite flotation. Miner Eng 2018;124:149–57. https://doi.org/10.1016/j.mineng.2018.05.022.

[6] Yuhua W, Jianwei R. The flotation of quartz from iron minerals with a combined quaternary ammonium salt. Int J Miner Process 2005;77:116–22. https://doi.org/10.1016/j.minpro.2005.03.001.

[7] Zhang C, Tan Y, Yin F, Wu J, Wang L, Cao J. The influence of branched chain length on different causticized starches for the depression of serpentine in the flotation of pentlandite. Minerals 2022;12:1081. https://doi.org/10.3390/min12091081.

[8] Alcázar-Alay SC, Meireles MAA. Physicochemical properties, modifications and applications of starches from different botanical sources. Food Sci Technol 2015;35:215–36. https://doi.org/10.1590/1678-457X.6749.

[9] Cao P, Wu G, Yao Z, Wang Z, Li E, Yu S, et al. Effects of amylose and amylopectin molecular structures on starch electrospinning. Carbohydr Polym 2022;296:119959. https://doi.org/10.1016/j.carbpol.2022.119959.

[10] Sandhu K, Singh N. Some properties of corn starches II: physicochemical, gelatinization, retrogradation, pasting and gel textural properties. Food Chem 2007;101:1499–507. https://doi.org/10.1016/j.foodchem.2006.01.060.

[11] Wang S, Wang J, Wang S, Wang S. Annealing improves paste viscosity and stability of starch. Food Hydrocoll 2017;62:203–11. https://doi.org/10.1016/j.foodhyd.2016.08.006.

[12] Qi X, Tong X, Pan W, Zeng Q, You S, Shen J. Recent advances in polysaccharide-based adsorbents for wastewater treatment. J Clean Prod 2021;315:128221. https://doi.org/10.1016/j.jclepro.2021.128221.

[13] Bello-Perez LA, Paredes-Lopez O, Roger P, Colona P. Molecular characterization of some amylopectins. Cereal Chem 1996;73:12–7.

[14] Cornell HJ. The effect of amylopectin on the properties of starch gels. Starch - Stärke 1963;15:43–50. https://doi.org/10.1002/star.19630150202.

[15] Laskowski JS, Liu Q, O'Connor CT. Current understanding of the mechanism of polysaccharide adsorption at the mineral/aqueous solution interface. Int J Miner Process 2007;84:59–68. https://doi.org/10.1016/j.minpro.2007.03.006.

[16] Roger P, Bello-Perez LA, Colonna P. Contribution of amylose and amylopectin to the light scattering behaviour of starches in aqueous solution. Polymer 1999;40:6897–909.

[17] Rolland-Sabaté A, Guilois S, Jaillais B, Colonna P. Molecular size and mass distributions of native starches using complementary separation methods: asymmetrical flow field flow fractionation (A4F) and hydrodynamic and size exclusion chromatography (HDC-SEC). Anal Bioanal Chem 2011;399:1493–505. https://doi.org/10.1007/s00216-010-4208-4.

[18] Andrade EC, Chelgani SC, De Salles Leal Filho L. A systematic study on gelatinization efficiency of starch by NaOH for enhanced hematite depression. Miner Eng 2024;209:108621. https://doi.org/10.1016/j.mineng.2024.108621.

[19] Iwasaki I. Interaction of starch and calcium in soap flotation of activated silica from iron ores. Trans Am Inst Min Metall Pet Eng 1965;232:383–7.

[20] Pinto CLL, De Araujo AC, Peres AEC. The effect of starch, amylose and amylopectin on the depression of oxi-minerals. Miner Eng 1992;5:469–78. https://doi.org/10.1016/0892-6875(92)90226-Y.

[21] Silva AC, Silva EMS, Peres AEC, Sousa DN. Temperature influence in cornstarch gelatinization for froth flotation. REM - Int Eng J 2017;70:231–5. https://doi.org/10.1590/0370-44672016700085.

[22] Yang S, Li C, Wang L. Dissolution of starch and its role in the flotation separation of quartz from hematite. Powder Technol 2017;320:346–57. https://doi.org/10.1016/j.powtec.2017.07.061.

[23] Yang S, Wang L. Measurement of froth zone and collection zone recoveries with various starch depressants in anionic flotation of hematite and quartz. Miner Eng 2019;138:31–42. https://doi.org/10.1016/j.mineng.2019.04.027.

[24] Cornejo-Ramírez Y, Cinco-Moroyoqui F, Carvajal-Millán E, Brown-Bojórquez F, Rosas-Burgos E, Burgos-Hernández A, et al. Dynamic rheology and microstructure of starch gels affected by triticale genomic composition and developing stage. Int Agrophysics 2019;33:21–30. https://doi.org/10.31545/intagr/103752.

[25] Ismail H, Irani M, Ahmad Z. Starch-based hydrogels: present status and applications. Int J Polym Mater 2013;62:411–20. https://doi.org/10.1080/00914037.2012.719141.

[26] Sajilata MG, Singhal RS, Kulkarni PR. Resistant starch–A review. Compr Rev Food Sci Food Saf 2006;5:1–17. https://doi.org/10.1111/j.1541-4337.2006.tb00076.x.

[27] Nakhaei F, Irannajad M. Reagents types in flotation of iron oxide minerals: a review. Miner Process Extr Metall Rev 2018;39:89–124. https://doi.org/10.1080/08827508.2017.1391245.

[28] Roberts SA, Cameron RE. The effects of concentration and sodium hydroxide on the rheological properties of potato starch gelatinisation. Carbohydr Polym 2002;50:133–43. https://doi.org/10.1016/S0144-8617(02)00007-3.

[29] Singh N, Singh J, Kaur L, Singh Sodhi N, Singh Gill B. Morphological, thermal and rheological properties of starches from different botanical sources. Food Chem 2003;81:219–31. https://doi.org/10.1016/S0308-8146(02)00416-8.

[30] Chakraborty I, Pallen S, Shetty Y, Roy N, Mazumder N. Advanced microscopy techniques for revealing molecular structure of starch granules. Biophys Rev 2020;12:105–22. https://doi.org/10.1007/s12551-020-00614-7.

[31] Silva EMS, Peres AEC, Silva AC, Leal MCDM, Lião LM, Almeida VOD. Sorghum starch as depressant in mineral flotation: part 1 – extraction and characterization. J Mater Res Technol 2019;8:396–402. https://doi.org/10.1016/j.jmrt.2018.04.001.

[32] Tao J, Huang J, Yu L, Li Z, Liu H, Yuan B, et al. A new methodology combining microscopy observation with Artificial Neural Networks for the study of starch gelatinization. Food Hydrocoll 2018;74:151–8. https://doi.org/10.1016/j.foodhyd.2017.07.037.

[33] Rohem Peçanha E, Da Fonseca De Albuquerque MD, Antoun Simão R, De Salles Leal Filho L, De Mello Monte MB. Interaction forces between colloidal starch and quartz and hematite particles in mineral flotation. Colloids Surf A Physicochem Eng Asp 2019;562:79–85. https://doi.org/10.1016/j.colsurfa.2018.11.026.

[34] Hadjittofis E, Das SC, Zhang GGZ, Heng JYY. Interfacial phenomena. Dev. Solid oral dos. Forms. Elsevier; 2017. p. 225–52. https://doi.org/10.1016/B978-0-12-802447-8.00008-X.

[35] Israelachvili JN. Intermolecular and surface forces. third ed. Burlington (Mass: Academic press; 2011.

[36] Laskowski J, Ralston J, editors. Colloid chemistry in mineral processing. Amsterdam ; New York : New York, NY, U.S.A: Elsevier ; Distributors for the U.S. and Canada, Elsevier Science Pub. Co; 1992.

[37] Gomes De Sousa SR, Leonel A, Bombard AJF. On the Hamaker constant of the metallic iron, the retardation effect and their relevance in DLVO theory applied to oil-based magnetorheological fluid with 1-octylamine. Smart Mater Struct 2020;29:055039. https://doi.org/10.1088/1361-665X/ab6abe.

[38] Visser J. On Hamaker constants: A comparison between Hamaker constants and Lifshitz-van der Waals constants. Adv Colloid Interface Sci 1972;3:331–63. https://doi.org/10.1016/0001-8686(72)85001-2.

[39] Gunasekaran S, Ak MM. Dynamic oscillatory shear testing of foods — selected applications. Trends Food Sci Technol 2000;11:115–27. https://doi.org/10.1016/S0924-2244(00)00058-3.

[40] Kawabata A, Akuzawa S, Ishii Y, Yazaki T, Otsubo Y. Sol—gel transition and elasticity of starch. Biosci Biotechnol Biochem 1996;60:567–70. https://doi.org/10.1271/bbb.60.567.

[41] Rosalina I, Bhattacharya M. Dynamic rheological measurements and analysis of starch gels. Carbohydr Polym 2002;48:191–202. https://doi.org/10.1016/S0144-8617(01)00235-1.

[42] Teyssandier F, Cassagnau P, Gérard JF, Mignard N. Sol–gel transition and gelatinization kinetics of wheat starch. Carbohydr Polym 2011;83:400–6. https://doi.org/10.1016/j.carbpol.2010.07.061.

[43] Barnes HA. A handbook of elementary rheology. Aberystwyth: University of Wales Institute of Non-Newtonian Fluid Mechanics; 2000.

[44] Bernreitner K, Neiβ W, Gahleitner M. Correlation between molecular structure and rheological behaviour of polypropylene. Polym Test 1992;11:89–100. https://doi.org/10.1016/0142-9418(92)90040-I.

[45] Berry GC, Fox TG. The viscosity of polymers and their concentrated solutions. In: Fortschritte hochpolym.-forsch., 5/3. Berlin/Heidelberg: Springer-Verlag; 1968. p. 261–357. https://doi.org/10.1007/BFb0050985.

[46] Cross MM. Viscosity, molecular weight and chain entanglement. Polymer 1970;11:238–44. https://doi.org/10.1016/0032-3861(70)90034-0.

[47] Kwakye-Nimo S, Inn Y, Yu Y, Wood-Adams PM. Linear viscoelastic behavior of bimodal polyethylene. Rheol Acta 2022;61:373–86. https://doi.org/10.1007/s00397-022-01340-5.

[48] Mezger T. The rheology handbook: for users of rotational and oscillatory rheometers. 5th revised edition. Hannover: Vincentz; 2020.

[49] Sangroniz L, Fernández M, Santamaria A. Polymers and rheology: a tale of give and take. Polymer 2023;271:125811. https://doi.org/10.1016/j.polymer.2023.125811.

[50] Stadler FJ, Piel C, Kaschta J, Rulhoff S, Kaminsky W, Münstedt H. Dependence of the zero shear-rate viscosity and the viscosity function of linear high-density polyethylenes on the mass-average molar mass and polydispersity. Rheol Acta 2006;45:755–64. https://doi.org/10.1007/s00397-005-0042-6.

[51] Vega JF, Otegui J, Ramos J, Martínez-Salazar J. Effect of molecular weight distribution on Newtonian viscosity of linear polyethylene. Rheol Acta 2012;51:81–7. https://doi.org/10.1007/s00397-011-0594-6.

[52] Barnes HA, Walters K, Hutton JF. An introduction to rheology. Amsterdam Oxford New-York: Elsevier; 1989 [Etc.].

[53] Fu Z, Che L, Li D, Wang L, Adhikari B. Effect of partially gelatinized corn starch on the rheological properties of wheat dough. LWT - Food Sci Technol 2016;66:324–31. https://doi.org/10.1016/j.lwt.2015.10.052.

[54] Pietrzyk S, Juszczak L, Fortuna T, Ciemniewska A. Effect of the oxidation level of corn starch on its acetylation and physicochemical and rheological properties. J Food Eng 2014;120:50–6. https://doi.org/10.1016/j.jfoodeng.2013.07.013.

[55] Ramli H, Zainal NFA, Hess M, Chan CH. Basic principle and good practices of rheology for polymers for teachers and beginners. Chem Teach Int 2022;4:307–26. https://doi.org/10.1515/cti-2022-0010.

[56] Miri T. Viscosity and oscillatory rheology. In: Norton IT, Spyropoulos F, Cox P, editors. Pract. Food rheol. first ed. Wiley; 2011. p. 7–28. https://doi.org/10.1002/9781444391060.ch2.
[57] Steffe JF. Rheological methods in food process engineering, vol. 2. East Lansing: Freeman Press; 1996.
[58] Séne M, Thévenot C, Prioul JL. Simultaneous spectrophotometric determination of amylose and amylopectin in starch from maize kernel by multi-wavelength analysis. J Cereal Sci 1997;26:211–21. https://doi.org/10.1006/jcrs.1997.0124.
[59] Wang JP, Yu B, Xu X, Yang N, Jin Z, Kim JM. Orthogonal-function spectrophotometry for the measurement of amylose and amylopectin contents. Food Chem 2011;127:102–8. https://doi.org/10.1016/j.foodchem.2010.12.094.
[60] Eshtiaghi N, Markis F, Yap SD, Baudez J-C, Slatter P. Rheological characterisation of municipal sludge: a review. Water Res 2013;47:5493–510. https://doi.org/10.1016/j.watres.2013.07.001.
[61] Peker SM, Helvacı ŞŞ. Solid-liquid two phase flow. first ed. Amsterdam Oxford: Elsevier; 2008.
[62] van der Sman RGM, Ubbink J, Dupas-Langlet M, Kristiawan M, Siemons I. Scaling relations in rheology of concentrated starches and maltodextrins. Food Hydrocoll 2022;124:107306. https://doi.org/10.1016/j.foodhyd.2021.107306.
[63] Peres AEC, Correa MI. Depression of iron oxides with corn starches. Miner Eng 1996;9:1227–34. https://doi.org/10.1016/S0892-6875(96)00118-5.
[64] Yang S, Xu Y, Kang H, Li K, Li C. Investigation into starch adsorption on hematite and quartz in flotation: role of starch molecular structure. Appl Surf Sci 2023;623:157064. https://doi.org/10.1016/j.apsusc.2023.157064.
[65] Błaszczak W, Lewandowicz G. Light microscopy as a tool to evaluate the functionality of starch in food. Foods 2020;9:670. https://doi.org/10.3390/foods9050670.
[66] Yang S, Dhital S, Zhang M-N, Wang J, Chen Z-G. Structural, gelatinization, and rheological properties of heat-moisture treated potato starch with added salt and its application in potato starch noodles. Food Hydrocoll 2022;131:107802. https://doi.org/10.1016/j.foodhyd.2022.107802.
[67] Hussien A. Effect of enzymatic treatment of starch gelatinized with sodium hydroxide. Egypt J Chem 2020. https://doi.org/10.21608/ejchem.2020.27970.2607. 0:0–0.
[68] Juszczak L, Witczak M, Ziêba T, Fortuna T. Rheological behaviour of heated potato starch dispersions. Int Agrophysics 2012;26:381–6. https://doi.org/10.2478/v10247-012-0053-3.
[69] Morris ER, Cutler AN, Ross-Murphy SB, Rees DA, Price J. Concentration and shear rate dependence of viscosity in random coil polysaccharide solutions. Carbohydr Polym 1981;1:5–21. https://doi.org/10.1016/0144-8617(81)90011-4.
[70] Wu K, Dai S, Gan R, Corke H, Zhu F. Thermal and rheological properties of mung bean starch blends with potato, sweet potato, rice, and sorghum starches. Food Bioprocess Technol 2016;9:1408–21. https://doi.org/10.1007/s11947-016-1730-1.
[71] Xie F, Yu L, Su B, Liu P, Wang J, Liu H, et al. Rheological properties of starches with different amylose/amylopectin ratios. J Cereal Sci 2009;49:371–7. https://doi.org/10.1016/j.jcs.2009.01.002.
[72] Yousefi AR, Razavi SMA. Dynamic rheological properties of wheat starch gels as affected by chemical modification and concentration: rheology of wheat starch gels. Starch - Stärke 2015;67:567–76. https://doi.org/10.1002/star.201500005.
[73] Agwu OE, Akpabio JU, Ekpenyong ME, Inyang UG, Asuquo DE, Eyoh IJ, et al. A critical review of drilling mud rheological models. J Pet Sci Eng 2021;203:108659. https://doi.org/10.1016/j.petrol.2021.108659.
[74] Turian RM, Ma TW, Hsu FLG, Sung DJ. Flow of concentrated non-Newtonian slurries: 1. Friction losses in laminar, turbulent and transition flow through straight pipe. Int J Multiph Flow 1998;24:225–42. https://doi.org/10.1016/S0301-9322(97)00038-4.
[75] Tang M, Wang Y, Niu X, Liu D. Morphological characteristics of starch sol-gel and its influences on flocculation of fine particles. Miner Eng 2022;186:107745. https://doi.org/10.1016/j.mineng.2022.107745.
[76] Tang M, Liu Q. The acidity of caustic digested starch and its role in starch adsorption on mineral surfaces. Int J Miner Process 2012;112–113:94–100. https://doi.org/10.1016/j.minpro.2012.06.001.
[77] Mohamed AA, Alamri MS, Hussain S, Ibraheem MA, Qasem AA. Rheological properties of sweet potato starch-date syrup gel. Food Sci Technol 2019;39:1030–9. https://doi.org/10.1590/fst.16618.
[78] Choi D-W, Chang Y-H. Steady and dynamic shear rheological properties of buckwheat starch-galactomannan mixtures. Prev Nutr Food Sci 2012;17:192–6. https://doi.org/10.3746/pnf.2012.17.3.192.
[79] Von Borries-Medrano E, Jaime-Fonseca MR, Aguilar-Méndez MA. Tapioca starch-galactomannan systems: comparative studies of rheological and textural properties. Int J Biol Macromol 2019;122:1173–83. https://doi.org/10.1016/j.ijbiomac.2018.09.067.
[80] Yousefi AR, Ako K. Controlling the rheological properties of wheat starch gels using Lepidium perfoliatum seed gum in steady and dynamic shear. Int J Biol Macromol 2020;143:928–36. https://doi.org/10.1016/j.ijbiomac.2019.09.153.
[81] Moreira GF, Peçanha ER, Monte MBM, Leal Filho LS, Stavale F. XPS study on the mechanism of starch-hematite surface chemical complexation. Miner Eng 2017;110:96–103. https://doi.org/10.1016/j.mineng.2017.04.014.
[82] Weisseborn PK, Warren LJ, Dunn JG. yanh. Colloids Surf A Physicochem Eng Asp 1995;99:11–27. https://doi.org/10.1016/0927-7757(95)03111-P.
[83] Aparicio-Saguilán A, Méndez-Montealvo G, Solorza-Feria J, Bello-Pérez LA. Thermal and viscoelastic properties of starch gels from maize varieties. J Sci Food Agric 2006;86:1078–86. https://doi.org/10.1002/jsfa.2461.
[84] Ulbrich M, Wiesner I, Flöter E. Molecular characterization of acid-thinned wheat, potato and pea starches and correlation to gel properties. Starch - Stärke 2015;67:424–37. https://doi.org/10.1002/star.201400233.
[85] Gao X, Huang L, Xiu J, Yi L, Zhao Y. Evaluation of viscosity changes and rheological properties of diutan gum, xanthan gum, and scleroglucan in extreme reservoirs. Polymers 2023;15:4338. https://doi.org/10.3390/polym15214338.